

Highly Thermo-conductive Fluid with Boron Nitride Nanofillers

Chunyi Zhi,^{†,*} Yibin Xu,^{*} Yoshio Bando,[†] and Dmitri Golberg[†]

[†]International Center for Materials Nanoarchitectonics (MANA), National Institute for Materials Science (NIMS), Namiki 1-1, Tsukuba, Ibaraki 305-0044, Japan, and

^{*}Materials Information Technology Station, National Institute for Materials Science, Tokyo 153-0061, Japan

Boron nitride (BN) materials, which possess very similar structures with carbon materials, are attracting more and more attention owing to their constant and wide band gap independent of morphology,¹ superb mechanical properties,^{2,3} and marked chemical inertness.⁴ Moreover, as insulating materials with very high thermal conductivity,⁵ BN phases were always thought to be attractive for highly thermo-conductive insulating composite materials.^{6–8} However, it should be noted that for the layered BN materials, high thermal conductivity can only be obtained inside the (002) planes (up to hundreds to thousands of W/mK), whereas in other lattice planes, the thermal conductivity is not that impressive (several W/mK).⁹ Therefore, one of the important issues while using BN materials as thermo-conductive fillers is to maximize the positive effect of their (002) lattice planes, but to minimize the contribution of other planes.^{7,10} Fortunately, the layered structures of BN materials enable them to form nanotubular and nanospherical morphologies. This maximizes the exposure of (002) lattice planes and minimizes the effects of others on the thermal conductivity.

Heat transfer using fluids has had comprehensive applications in transport, electronic, and nuclear cooling systems, *etc.* Conventional fluids, such as water and engine oil are normally used for heat transfer. Many applications would benefit from an increase in thermal conductivity of a heat transferring fluid. Such improvement would result in downsizing heat transfer systems, lowering capital costs, and improving energy conversion efficiencies. In recent years, nanosized thermo-conductive particles have been tried in fluids for heat transfer improvement.¹¹ Usually, the particles adopted have been made of Al₂O₃,¹² CuO,¹³ SiC,¹⁴ TiO₂,¹⁵ carbon nanotubes (CNTs),¹⁶ or metals,^{17,18} *etc.* Studies on the dispersion of nanoparticles and theoretical modeling of nanofluids were also performed.^{19,20} On one hand, owing to many

ABSTRACT We report for the first time how boron nitride (BN) nanotubes and nanospheres may effectively be used to achieve remarkable thermal conductivity improvement of a fluid. Benefiting from high thermal conductivity and high-aspect-ratio of BN nanotubes, at a fraction of 6 vol %, the thermal conductivity of water was remarkably improved, up to ~2.6-times. With BN nanospheres as fillers, the viscosity of the fluid can be kept decently low and thermal conductivity can also be effectively improved. A combination of BN nanotubes and nanospheres was found to increase the fluid's thermal conductivity while keeping its viscosity low, thus, such mixtures can be promising fillers for highly thermo-conductive fluids. Finally, calculations based on finite element method were used to investigate the regarded nanofluids. On the basis of the results, thermal conductivity was estimated to be more than, or close to 200 W/mK for BN nanotubes and nanospheres, respectively.

KEYWORDS: BN nanotubes · BN nanospheres · thermal conductivity · fluid

experimental difficulties involved in accurate determination of the nanofluid's composition and morphology, and its thermal conductivity and viscosity, the true thermal conductivity values of nanofluids have been somewhat controversial.²¹ On the other hand, the reached so far practical improvements of the fluids' thermal conductivities are far from satisfactory, and new fillers are required for increasing cooling efficiencies.

In this article, for the first time, we present systematic studies on a water-based fluid using BN nanotubes (BNNTs) and BN nanospheres (BNNs) as nanofillers. Effective thermal conductivity improvement (up to ~2.6-fold) was obtained when BNNTs were used, which is attributed to their fibrous structures and high-aspect-ratios. The advantage of BNNs as nanofillers was their ability to also improve thermal conductivity of water but at the same time to keep its viscosity low. Subsequently, by combining BNNTs and BNNs as mixed fillers, a fluid with thermal conductivity of 1.21 W/mK and decently low viscosity of 2.0 Pas was designed. Finally, finite element method (FEM) calculations were performed for the data analysis. On the basis of the calculations, the BNNTs were found to possess thermal conductivity of more

* Address correspondence to ZHI.Chunyi@nims.go.jp.

Received for review May 26, 2011 and accepted July 13, 2011.

Published online July 13, 2011
10.1021/nn201946x

© 2011 American Chemical Society

than 200 W/mK, and the BNNSs' thermal conductivity was determined to be close to 200 W/mK.

RESULTS AND DISCUSSION

As shown in Figure 1a, the as-grown purified BNNTs possess long fibrous structures. Their diameter is around 50 nm and the length can be up to tens of micrometers.^{22,23} To improve their affinity with solvents, the BNNTs were dispersed in hydrogen peroxide by magnetic stirring for 24 h at room temperature, followed by oxidation at 90 °C in an autoclave for 24 h. As reported before, the treated BNNTs are hydroxylated and can be well dispersed in water at a low concentration.²⁴ However, it should be noted that long-term stirring can shorten the BNNTs. As shown in Figure 1b, the stirred BNNTs possess lengths of around several micrometers and the average aspect ratio is *ca.* 40–200 after stirring and hydroxylation processes. To minimize the surface energy, they tend to assemble into the nematically ordered structures.²⁵ Figure 1c shows the as-prepared BNNSs that exhibit diameters of hundreds of nanometers.²⁶

Transmission electron microscopy (TEM) data acquired on BNNTs/BNNSs are shown in Figure 2. Well-defined tubular structures are documented for BNNTs. Moreover, BNNTs are perfectly straight, which is due to ionic characters of B–N bonds and a low defect concentration under a high temperature growth.²⁷ High-resolution TEM images show well-crystallized BNNTs with a so-called double-helix structure.²⁸ The traces of an amorphous-like boron oxide material can be observed on the BNNTs' surfaces. Figures 2 (c and d) show that BNNSs possess well-defined spherical morphologies. Under high resolution TEM the lattice fringes can be clearly resolved; however, the crystallization is not perfect due to the relatively low growth temperature.²⁸

To utilize the nanoparticles for improvement of the thermal conductivity of a fluid, one important issue is to obtain a stable suspension. Although the hydroxylated BNNTs and as-grown BNNSs can be well dispersed in water at low concentrations, it is difficult to stabilize such dispersions at high concentrations. Therefore, in our experiments, polydiallyldimethylammonium chloride (PDPA) was used as a surfactant. There are positively charged functional groups on the skeleton of the PDPA; by contrast the surface of the BN nanomaterial is negatively charged, which may be due to –OH groups. Therefore, electro-static interactions lead to the effective absorption of PDPA on BN nanomaterials.^{29,30} Two kinds of PDPA were purchased from Aldrich Company. Their molecular weights were 100 000–200 000 and 200 000–350 000, respectively. To prove strong interactions between PDPA and BN nanofillers, BNNTs/BNNSs were put into a 20 wt % PDPA aqueous solution and stirred for 5 h at room temperature, followed by

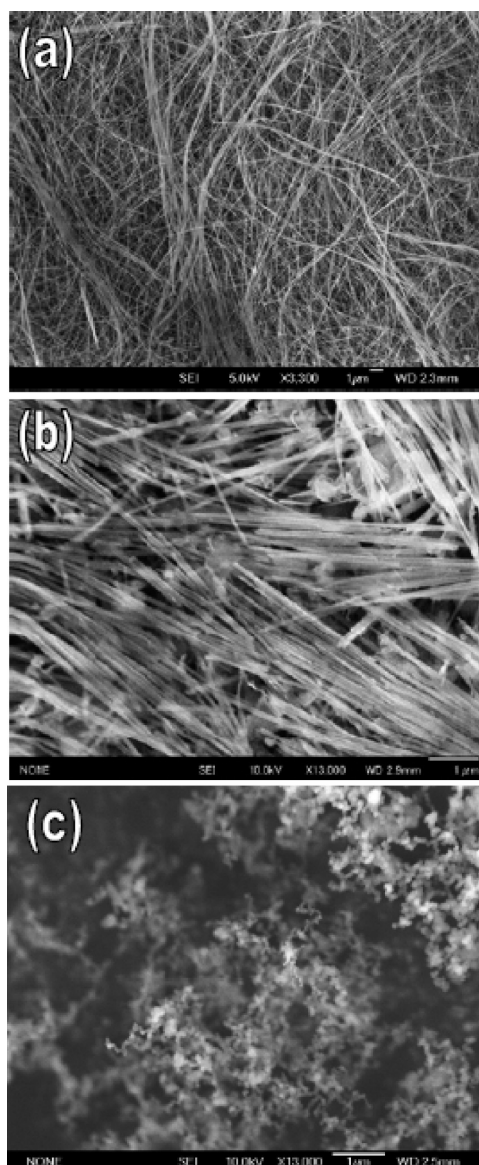


Figure 1. (a and b) SEM images of purified BNNTs and hydroxylated BNNTs; the hydroxylated BNNTs are shortened to around 5 μm due to magnetic stirring; (c) SEM image of BNNSs.

separation under centrifugation. Zeta-potential measurements were used to investigate the surface charge status of pristine BNNTs/BNNSs and their PDPA composites. The results are shown in Figure 3. It is clear that pristine BNNTs/BNNSs have negatively charged surfaces, which make positively charged PDPA bind to them easily. PDPA with a larger molecular weight was found to be more effective: higher positive zeta potentials were measured for BN nanomaterials modified with PDPA of 200 000–350 000 molecular weight. It is suggested that molecules with high molecular weight have longer polymer chains, which can actually cover the surface of the BN nanomaterials more effectively. The effective interactions were also verified by TEM observations. The solution of PDPA/BNNSs and PDPA/BNNTs were dropped on a copper grid, followed by drying

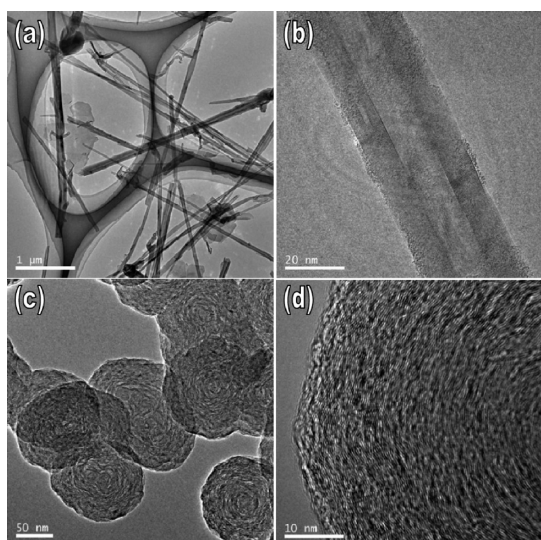


Figure 2. (a and c) Low magnification TEM images of BNNTs and BNNSs; (b and d) high resolution TEM images of BNNTs and BNNSs, which indicate better crystallization of BNNTs compared to BNNSs due to higher synthesis temperature.

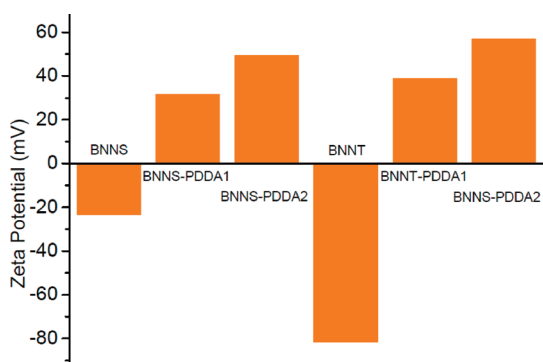


Figure 3. Zeta potential results of BNNTs/BNNSs and PDDA modified BNNTs/BNNSs. It should be noted that PDDA 1 is PDDA with a molecular weight *ca.* 100 000–200 000, and PDDA 2 is PDDA with a molecular weight *ca.* 200 000–350 000. The results indicate that BN nanofillers can strongly interact with PDDA.

before the TEM measurements. As shown in Figure 4, the polymer is tightly attached on the BN nanomaterials, no voids can be observed. Even when the BNNTs/BNNSs extrude out of the PDDA matrix, their surfaces are still covered with the amorphous PDDA layer. These observations indicate intensive electrostatic interactions between BN nanomaterials and PDDA, as expected. Thus PDDA can effectively be utilized for stabilizing BNNT/BNNS suspensions with a high nanofiller concentration.

For fabricating stable suspensions of BNNTs/BNNSs, 20 wt % PDDA with a molecular weight of 200 000–350 000 was used. We found that 20 wt % PDDA is a good choice: it is sticky enough to stabilize a suspension of BN nanomaterials, but the viscosity is not too high. Five hours of stirring was found to be enough to disperse BN nanomaterials. It should be noted that the

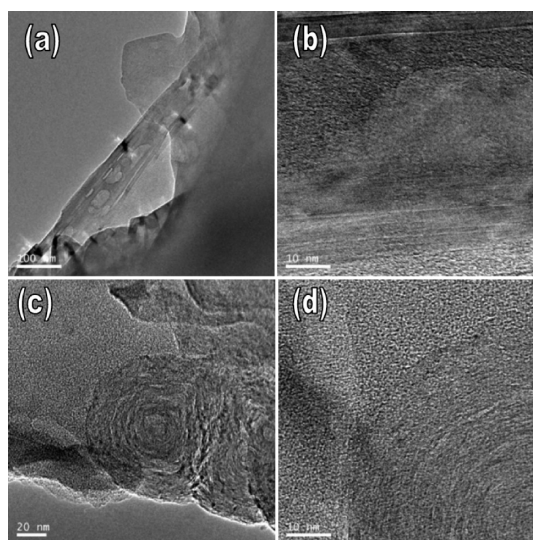


Figure 4. (a and b) TEM images of BNNTs-PDDA composites; (c and d) TEM images of BNNSs-PDDA composites. Amorphous layers can be found on the surfaces of BNNTs/BNNSs, which result from strong electrostatic interactions between BNNT/BNNS and PDDA.

viscosity was used not only to stabilize the suspension, but also to minimize convection in the fluid, which can avoid errors during the thermal conductivity measurements. The densities of the BN nanofillers were estimated based on their structures. Certain amounts of BN nanofillers were added to PDDA aqueous solutions and magnetically stirred for 24 h to form suspensions with 0.6 vol %, 2.0 vol %, 3 vol %, 4.5 vol %, and 6 vol % BN nanofiller fractions.

Thermal conductivities were measured using a hot-disk method.³¹ A disk sensor was placed inside a \sim 50 mL fluid fabricated and then heated by a constant electrical current for a short period of time. The generated heat dissipates from the sensor into the surrounding fluid, causing a rise in temperature of the sensor and the fluid. The average transient temperature increase of the sensor was simultaneously measured by monitoring the change in electrical resistance. The temperature coefficient of resistivity of the sensor material correlates with the change in resistivity under the corresponding change in temperature. This fact was used to accurately and finally calculate the thermal conductivity. The sensor was mounted on a lampstand to keep it in plane and then submerged into the fluid. For every sample, the thermal conductivity was measured 10 times to calculate an average value and mean-square deviation (see Supporting Information for diagram). It should be noted that attachment of nanoparticles on sensors may induce some potential errors. However, since the thermal penetration depth was >1 cm, it is believed that such influence was negligible. It is also noted that hot-disk methods have already been comprehensively used for thermal conductivity measurement of nanofluids and their

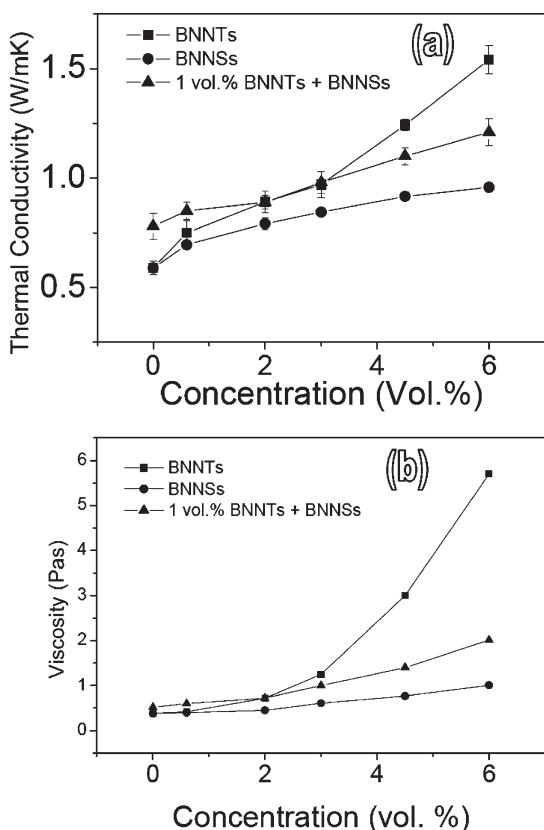


Figure 5. (a and b) Thermal conductivity and viscosity of a nanofluid with BN nanofillers. The curves marked with triangles correspond to the samples using fillers made of 1 vol % BNNTs and variable contents of BNNs.

applicability has been verified.^{32,33} TVB-10 viscometer was used for viscosity measurement and the measurement principle is presented in the Supporting Information.

The BNNTs/BNNs were found to effectively improve thermal conductivity of water. As shown in Figure 5, water with 20 wt % PDDA possesses thermal conductivity of 0.59 W/mK, which is close to that of pure water. With up to 6 vol % BN nanofillers, the thermal conductivity increases to 1.54 W/mK (ca. 2.6-fold increase) for BNNTs and 0.95 W/mK (~1.6-fold increase) for BNNs. As expected, BNNTs are much more effective for thermal conductivity improvement, which is due to their fibrous structures and an ease in making the continuous heat transfer interchannel *via* multiple contacts between the tubes. At low filler fractions, the contacts may form short-range thermal transfer channels, which are absent in the case of BNNs, as schematically demonstrated in Figure 6. In addition, as a result of higher synthesis temperature, BNNTs possess better crystallization than BNNs. Since phonons are responsible for a thermal transfer in BN materials, better crystallization would result in less phonon scattering and a longer scattering mean free path. This means that BNNTs should have higher thermal conductivity and can more effectively improve thermal conductivity of a matrix than BNNs. However, it should

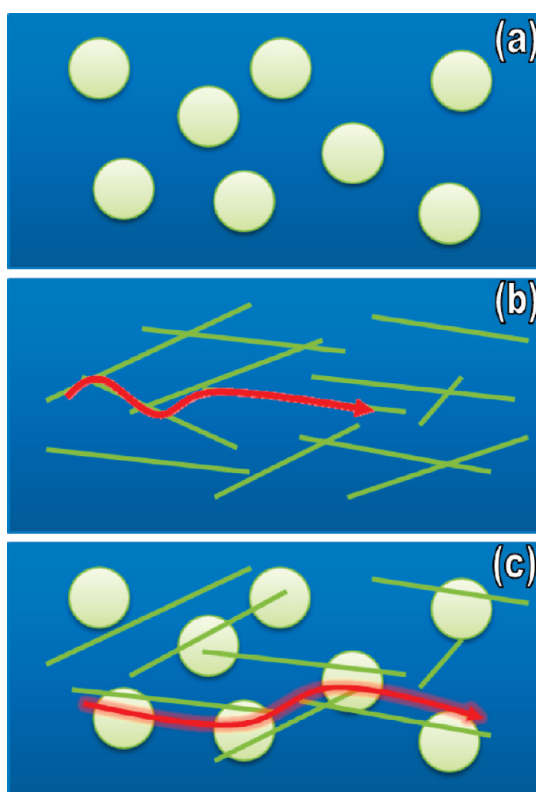


Figure 6. Schematics for the formation of a thermal transfer channel in composites. One-dimensional fillers can form effective thermal transfer channels easier, while the combination of spheres and fibrous fillers may have an advantage of both high thermal conductivity and low viscosity.

be noted that, as shown in Figure 5b, the fibrous structures of BNNTs also induce a dramatic increase in viscosity of the fluid, while embedding of BNNs may keep the fluid at a relatively low viscosity. To combine the effective thermal conductivity improvement of BNNTs and low viscosity maintaining by BNNs, composite fillers made of BNNTs and BNNs mixtures were designed. As shown in Figure 6c, a small amount of BNNTs may bridge BNN particles to form an effective thermal transfer pathway, while the viscosity is expected to be maintained relatively low. The experimental results are depicted in Figure 5. As expected, with 1 vol % extra BNNTs added, the thermal conductivity was improved to 1.21 W/mK with 6 vol % BNNs, while the viscosity was kept much lower than in the case when only pure BNNT fillers were embedded. Therefore, compared with a case of utilizing one kind of filler with a high-aspect-ratio (to simply achieve high thermal conductivity of the nanofluid) the combination of fibrous BNNTs and spherical BNNs is thought to be an effective solution toward creation of a thermoconductive fluid with decently low viscosity. For example, the thermal conductivity and viscosity of fluid with 6 vol % BNNs + 1 vol % BNNTs are 1.21 W/mK and 2.0 Pas, respectively, while for fluid with 6 vol % BNNTs, they are 1.54 W/mK and 5.7 Pas, respectively. It is clear that with pure BNNTs, although higher

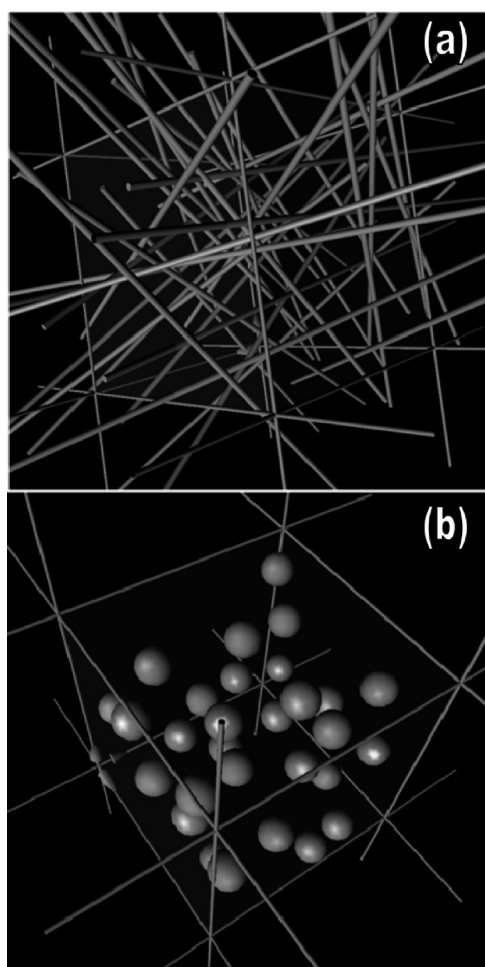


Figure 7. Composite models generated for FEM calculations. The filler fraction is 3 vol % for each model.

thermal conductivity was achieved, the increase in viscosity was disadvantageous.

Thermal conductivity improvement achieved by combined BNNTs/BNNSs fillers is remarkable compared with that achieved by Al_2O_3 , SiC, and CuO fillers, etc.^{12–16} This fact may result from their unique structures, very high thermal conductivity and good affinity to PDPA. In the literature, the fraction of fillers used was usually in the range of 0.1 vol % to 15 vol %, and the improvements achieved were mostly below 1.5-times of the thermal conductivity of a starting matrix (note that they are ~ 2.6 and ~ 1.6 for the present BNNTs and BNNSs, respectively).¹¹ For example, Wang *et al.* used 6.2 vol % to 14.8 vol % CuO in the ethylene glycol fluid, and an improvement of 1.24 to 1.54-times was obtained.¹² Works by Li *et al.* revealed that 2 vol % to 10 vol % Al_2O_3 in water could result in 1.15 to 1.22-fold improvement of thermal conductivity.³⁴ Actually the morphology effect can also be clearly seen from the literature data. CNTs were found to be much more effective than traditional Al_2O_3 and CuO particles, etc. Liu *et al.* reported that using 1 vol % CNTs, thermal conductivity of ethylene glycol could be improved

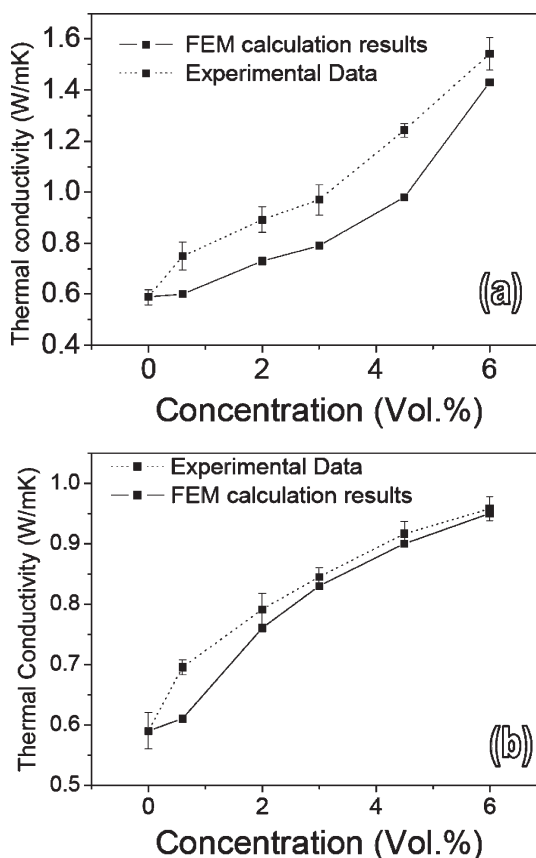


Figure 8. Comparison of fluid's thermal conductivity obtained under FEM calculations and experiments, which indicates that BNNTs may possess a thermal conductivity >200 W/mK, while the thermal conductivity of BNNSs may be close to 200 W/mK.

1.12-fold.³⁵ In the Marquis's study, very long CNTs were used and with 0.25 vol % to 1 vol % CNT fillers, the thermal conductivity of polyalphaolefin was improved 1.30 to 2.17-fold.³⁶ It should be noticed that when CNTs are used, the fluid will become not only thermoconductive but also electrically conductive. In the case when electrically insulating fluids are needed, BN nanofillers are undoubtedly preferable.

There have been many theoretical models developed for the prediction of thermal properties of composite materials, such as Agari model,³⁷ Every model,³⁸ Hatta model,³⁹ etc. However, these analytical solutions have always been deduced with specific simplifications, as well as keeping in mind the material properties and composite structures limitations. The finite element model (FEM) is a general method which can be used to calculate effective thermal conductivity of a heterogeneous materials system without the restrictions that the conventional analytical methods have. Therefore, FEM was selected to calculate the present composite systems. The purpose of our calculations was to demonstrate the efficiency of BN nanofillers for thermal conductivity improvement of a matrix. Moreover, since it is very difficult to measure thermal conductivity of BN nanofillers experimentally, our

calculations were also used to estimate thermal conductivity of BN nanofillers theoretically.

A FEM calculation system developed by the National Institute for Materials Science (NIMS), Japan, was employed.^{40,41} As indicated in the SEM images in Figure 1, BNNTs are defined as the tubes with the ratio of inner diameter/outer diameter/length = 1:2:200. Considering the previous experimental results in regard of BNNT thermal conductivity, a value of 200 W/mK was used for BNNTs and for the axis direction of BNNTs.⁴² Uniform voxel meshes with $45 \times 45 \times 45$ were adopted. The size of the composite model was set to be $2 \mu\text{m} \times 2 \mu\text{m} \times 2 \mu\text{m}$, and the number of particles and filler fractions were adjusted to make the diameter of BNNTs and BNNTs to be around 50 and 200 nm, respectively, which are close to the experimental observations. As a demonstration, the models generated with 3 vol % fillers are displayed in Figure 7.

As shown in Figure 8, unlike traditional calculation results using theoretical models, which usually give a well-defined shape of curves (such as linear dependence between filler fraction and thermal conductivity) the results of our calculations are fluctuant due to some degree of randomness of the structure models built. The calculation results are believed to be closer to reality. For BNNTs, the computed values (solid line) are generally lower than our experimental data (dashed line), which may indicate that a thermal conductivity of BNNTs is actually higher than the input value of 200 W/mK. In the case of BNNTs, the two curves are very close, which may imply that the thermal conductivity of BNNTs is indeed close to 200 W/mK. This is consistent with our previous discussions pointing out

that the better crystallization of BNNTs induces a longer phonon scattering mean free path, that results in a higher thermal conductivity of BNNTs as compared to that of BNNTs.

CONCLUSIONS

In summary, for the first time, we adopted BNNTs and BNNTs for fabrication of a highly thermo-conductive fluid. PDDA was found to intensively interact with BN nanofillers and effectively stabilize their suspensions at relatively high concentrations. Remarkable improvements of thermal conductivity of water were achieved: with 6 vol % fraction of BNNTs and BNNTs, thermal conductivity improvement was ~2.6-fold and 1.6-fold, respectively. These data indicate that BN nanofillers could be much more effective species than traditional CuO, MgO, and Al₂O₃ nanoparticles previously used as fillers. Due to higher thermal conductivity and aspect ratios, BNNTs exhibit higher efficiency for thermal conductivity improvement compared with BNNTs. In addition, a mixed combination of BNNTs and BNNTs fillers was found to be particularly effective: it results in a significant improvement of the fluid thermal conductivity while keeping its viscosity decently low. FEM calculations were used to investigate the nanofluids fabricated. According to them, BNNTs may possess thermal conductivity higher than 200 W/mK, whereas thermal conductivity of BNNTs is close to 200 W/mK. Our studies indicate that compared with traditional nanofillers BN nanofillers with maximally exposed (002) planes, for example, nanotubes and nanospheres, are very promising in the field of thermo-conductive fluids.

MATERIALS AND METHODS

The BNNTs used in this work were synthesized by a chemical vapor deposition method using boron and oxide as reactants at around 1500 °C. BNNTs used in the experiments were synthesized by a chemical vapor deposition reaction between B(OMe)₃ and ammonia at 900 °C, followed by high-temperature annealing. The detailed synthesis procedure was reported previously.^{19,20,23}

A scanning electron microscope (JEOL SM67F) was used to characterize the BNNTs. The microstructures were analyzed using a JEOL-3000F high-resolution field-emission TEM operated at 300 kV. Thermal conductivity measurements were performed using a hot-disk thermal constant analyzer (Kyoto Electronics, Japan) and the thermal conductivities of fluids were measured 10 times with a time interval between measurements of 20 min. A hot disk sensor with mica insulation and a radius of 14.65 mm was adopted. The sensor was immersed in 50 mL of a fluid for measurement. The thermal penetration depth was estimated to be around 1.3 cm. Therefore, the total fluid volume involved in the measurement was approximately 17 mL. Calibrations were performed before every batch of measurements to obtain the sensor thermal conductivity. However, since there was no standard calibration process designed for the measurements on nanoparticle suspensions for the regarded machine, we measured thermal

conductivity of some standard fluids, such as water, etc. These measurements indicated that the machine is applicable for the reliable thermal conductivity measurements of a fluid. TVB-10 viscometer (Toki Sangyo Company) was used for viscosity measurement.

Supporting Information Available: Details of thermal conductivity and viscosity measurements. This material is available free of charge via the Internet at <http://pubs.acs.org>.

REFERENCES AND NOTES

- Blase, X.; Rubio, A.; Louie, S. G.; Cohen, M. L. Stability and Band-Gap Constancy of Boron–Nitride Nanotubes. *Europhys. Lett.* **1994**, *28*, 335–340.
- Golberg, D.; Costa, P.; Lourie, O.; Mitome, M.; Bai, X. D.; Kurashima, K.; Zhi, C. Y.; Tang, C. C.; Bando, Y. Direct Force Measurements and Kinking under Elastic Deformation of Individual Multiwalled Boron Nitride Nanotubes. *Nano Lett.* **2007**, *7*, 2146–2151.
- Zhi, C. Y.; Bando, Y.; Tang, C. C.; Honda, S.; Kuwahara, H.; Golberg, D. Boron Nitride Nanotubes/Polystyrene Composites. *J. Mater. Res.* **2006**, *21*, 2794–2800.
- Chen, Y.; Zou, J.; Campbell, S. J.; Le Caer, G. Boron Nitride Nanotubes: Pronounced Resistance to Oxidation. *Appl. Phys. Lett.* **2004**, *84*, 2430–2432.

5. Chang, C. W.; Fennimore, A. M.; Afanasiev, A.; Okawa, D.; Ikuno, T.; Garcia, H.; Li, D. Y.; Majumdar, A.; Zettl, A. Isotope Effect on The Thermal Conductivity of Boron Nitride Nanotubes. *Phys. Rev. Lett.* **2006**, *97*, 085901.
6. Zhi, C. Y.; Bando, Y.; Tang, C. C.; Golberg, D. Boron Nitride Nanotubes. *Mater. Sci. Eng. Res.* **2010**, *70*, 92–111.
7. Gao, R.; Yin, L. W.; Wang, C. X.; Qi, Y. X.; Lun, N.; Zhang, L. Y.; Liu, Y. X.; Kang, L.; Wang, X. F. High-Yield Synthesis of Boron Nitride Nanosheets with Strong Ultraviolet Cathodoluminescence Emission. *J. Phys. Chem. C* **2009**, *113*, 15160–15165.
8. Yu, J.; Qin, L.; Hao, Y. F.; Kuang, S.; Bai, X. D.; Chong, Y. M.; Zhang, W. J.; Wang, E. Vertically Aligned Boron Nitride Nanosheets: Chemical Vapor Synthesis, Ultraviolet Light Emission, and Superhydrophobicity. *ACS Nano* **2010**, *4*, 414–422.
9. Kumar, A.; Pal, D. Lattice Thermal-Conductivity of Boron-Nitride Crystals at Temperatures 1.5 to 300 K. *Phys. Status Solidi B* **1985**, *129*, K9–K12.
10. Zhi, C. Y.; Bando, Y.; Terao, T.; Tang, C. C.; Kuwahara, H.; Golberg, D. Towards Thermoconductive, Electrically Insulating Polymeric Composites with Boron Nitride Nanotubes as Fillers. *Adv. Funct. Mater.* **2009**, *19*, 1857–1862.
11. Yu, W. H.; France, D. M.; Roubort, J. L.; Choi, S. U. S. Review and Comparison of Nanofluid Thermal Conductivity and Heat Transfer Enhancements. *Heat Transfer Eng.* **2008**, *29*, 432–460 and references therein.
12. Wang, X. W.; Xu, X. F.; Choi, S. U. S. Thermal Conductivity of Nanoparticle-Fluid Mixture. *J. Thermophys. Heat Transfer* **1999**, *13*, 474–480 and references therein.
13. Chang, M. H.; Liu, H. S.; Tai, C. Y. Preparation of Copper Oxide Nanoparticles and Its Application in Nanofluid. *Powder Technol.* **2011**, *207*, 378–386.
14. Xie, H.; Wang, J.; Xi, T.; Liu, Y. Thermal Conductivity of Suspensions Containing Nanosized SiC Particles. *Int. J. Thermophys.* **2002**, *23*, 571–580.
15. Murshed, S. M. S.; Leong, K. C.; Yang, C. Enhanced Thermal Conductivity of TiO₂-Water Based Nanofluids. *Int. J. Ther. Sci.* **2005**, *44*, 367–373.
16. Choi, S. U. S.; Zhang, Z. G.; Yu, W.; Lockwood, F. E.; Grulke, E. A. Anomalous Thermal Conductivity Enhancement in Nanotube Suspensions. *Appl. Phys. Lett.* **2001**, *79*, 2252–2254.
17. Hong, K. S.; Hong, T. K.; Yang, H. S. Thermal Conductivity of Fe Nanofluids Depending on The Cluster Size of Nanoparticles. *Appl. Phys. Lett.* **2006**, *88*, 031901.
18. Patel, H. E.; Das, S. K.; Sundararajan, T.; Sreekumaran Nair, A.; George, B.; Pradeep, T. Thermal Conductivities of Naked and Monolayer Protected Metal Nanoparticle Based Nanofluids: Manifestation of Anomalous Enhancement and Chemical Effects. *Appl. Phys. Lett.* **2003**, *83*, 2931–2933.
19. Chakraborty, S.; Saha, S. K.; Pandey, J. C.; Das, S. Experimental Characterization of Concentration of Nanofluid by Ultrasonic Technique. *Powder Technol.* **2011**, *210*, 304–307.
20. Mehta, S.; Chauhan, K. P.; Kanagaraj, S. Modeling of Thermal Conductivity of Nanofluids by Modifying Maxwell's Equation Using Cell Model Approach. *J. Nanopart. Res.* **2011**, *13*, 2791–2798.
21. Buongiorno, J.; Venerus, D. C.; Prabhat, N.; McKrell, T.; Townsend, J.; Christianson, R.; Tolmachev, Y. V.; Keblinski, P.; Hu, L. W.; Alvarado, J. L.; *et al.* A Benchmark Study on the Thermal Conductivity of Nanofluids. *J. Appl. Phys.* **2009**, *106*, 094312 and references therein.
22. Zhi, C. Y.; Bando, Y.; Tan, C. C.; Golberg, D. Effective Precursor for High Yield Synthesis of Pure BN Nanotubes. *Solid State Commun.* **2005**, *135*, 67–70.
23. Tang, C.; Bando, Y.; Sato, T.; Kurashima, K. A Novel Precursor for Synthesis of Pure Boron Nitride Nanotubes. *Chem. Commun.* **2002**, 1290–1291.
24. Zhi, C. Y.; Bando, Y.; Terao, T.; Tang, C. C.; Kuwahara, H.; Golberg, D. Chemically Activated Boron Nitride Nanotubes. *Asia. Chem.* **2009**, *4*, 1536–1540.
25. Zhi, C.; Bando, Y.; Wang, W.; Tang, C.; Kuwahara, H.; Golberg, D. DNA-Mediated Assembly of Boron Nitride Nanotubes. *Asia. Chem.* **2007**, *2*, 1581–1585.
26. Tang, C. C.; Bando, Y.; Huang, Y.; Zhi, C. Y.; Golberg, D. Synthetic Routes and Formation Mechanisms of Spherical Boron Nitride Nanoparticles. *Adv. Funct. Mater.* **2008**, *18*, 3653–3661.
27. Golberg, D.; Bando, Y.; Tang, C. C.; Zhi, C. Y. Boron Nitride Nanotubes. *Adv. Mater.* **2007**, *19*, 2413–2432.
28. Celik-Aktas, A.; Zuo, J. M.; Stubbins, J. F.; Tang, C. C.; Bando, Y. Double-Helix Structure in Multiwall Boron Nitride Nanotubes. *Acta Crystallogr., Sect. A* **2005**, *61*, 533–541.
29. Chen, H. J.; Wang, Y. L.; Wang, Y. Z.; Dong, S. J.; Wang, E. K. One-Step Preparation and Characterization of PDDA-Protected Gold Nanoparticles. *Polymer* **2006**, *47*, 763–766.
30. Marcelo, G.; Tarazona, M. P.; Saiz, E. Solution Properties of Poly (diallyldimethylammonium chloride) (PDDA). *Polymer* **2005**, *46*, 2584–2594.
31. Log, T.; Gustafsson, S. E. Transient Plane Source Technique for Measuring Thermal Transport Properties of Building Materials. *Fire Mater.* **1995**, *19*, 43–49.
32. Hu, P.; Shan, W. L.; Yu, F.; Chen, Z. S. Thermal Conductivity of AlN-Ethanol Nanofluids. *In. J. Thermophys.* **2008**, *29*, 1968–1973.
33. Li, X. F.; Zhu, D. S.; Wang, X. J.; Wang, N.; Gao, J. W. Thermal Conductivity Enhancement for Aqueous Alumina Nanosuspensions in the Presence of Surfactant. *J. Enhanced Heat Transfer* **2009**, *16*, 93–102.
34. Li, C. H.; Peterson, G. P. Experimental Investigation of Temperature and Volume Fraction Variations on the Effective Thermal Conductivity of Nanoparticle Suspensions (Nanofluids). *J. Appl. Phys.* **2006**, *99*, 084314.
35. Liu, M. S.; Lin, M. C. C.; Huang, I. T.; Wang, C. C. Enhancement of Thermal Conductivity with Carbon Nanotube for Nanofluids. *Int. Commun. Heat Mass Transfer* **2005**, *32*, 1202–1210.
36. Marquis, F. D. S.; Chibante, L. P. F. Improving The Heat Transfer of Nanofluids and Nanolubricants with Carbon Nanotubes. *J. Miner., Metal, Mater. Soc.* **2005**, *57*, 32–43.
37. Agari, Y.; Uno, T. Estimation on Thermal-conductivity of Filled Polymers. *J. Appl. Polym. Sci.* **1986**, *32*, 5705–5712.
38. Every, A. G.; Tzou, Y.; Hasselman, D. P. H.; Raj, R. The Effect of Particle-Size on The Thermal Conductivity of ZnS Diamond Composites. *Acta Metall. Mater.* **1992**, *40*, 123–129.
39. Hatta, H.; Taya, M. Effective Thermal Conductivity of a Misoriented Short Fiber Composite. *J. Appl. Phys.* **1985**, *58*, 2478–2486.
40. Xu, Y. B.; Yagi, K. Calculation of the Thermal Conductivity of Randomly Dispersed Composites Using a Finite Element Modelling Method. *Mater. Trans.* **2004**, *45*, 2602–2605.
41. Xu, Y. B.; Yagi, K. Automatic FEM Model Generation for Evaluating Thermal Conductivity of Composite with Random Materials Arrangement. *Comput. Mater. Sci.* **2004**, *30*, 242–250.
42. Zettl, A.; Chang, C. W.; Begtrup, G. A New Look at Thermal Properties of Nanotubes. *Phys. Status Solidi B* **2007**, *244*, 4181–4183.